Earth and Planetary Science Letters 403 (2014) 217–224

Contents lists available at ScienceDirect

Earth and Planetary Science Letters

www.elsevier.com/locate/epsl

Spectral masking of goethite in abandoned mine drainage systems: Implications for Mars

Selby Cull [a,*], Charles A. Cravotta III [b], Julia Grace Klinges [c], Chloe Weeks [a]

[a] Department of Geology, Bryn Mawr College, 101 Merion Avenue, Bryn Mawr, PA 19010, United States
[b] U.S. Geological Survey, Pennsylvania Water Science Center, New Cumberland, PA 17070, United States
[c] Haverford College, Haverford, PA 19041, United States

ARTICLE INFO

Article history:
Received 15 January 2014
Received in revised form 18 June 2014
Accepted 26 June 2014
Available online 24 July 2014
Editor: C. Sotin

Keywords:
Mars
remote sensing
acid mine drainage

ABSTRACT

Remote sensing studies of the surface of Mars use visible- to near-infrared (VNIR) spectroscopy to identify hydrated and hydroxylated minerals, which can be used to constrain past environmental conditions on the surface of Mars. However, due to differences in optical properties, some hydrated phases can mask others in VNIR spectra, complicating environmental interpretations. Here, we examine the role of masking in VNIR spectra of natural precipitates of ferrihydrite, schwertmannite, and goethite from abandoned mine drainage (AMD) systems in southeastern Pennsylvania. Mixtures of ferrihydrite, schwertmannite, and goethite were identified in four AMD sites by using X-ray diffractometry (XRD), and their XRD patterns compared to their VNIR spectra. We find that both ferrihydrite and schwertmannite can mask goethite in VNIR spectra of natural AMD precipitates. These findings suggest that care should be taken in interpreting environments on Mars where ferrihydrite, schwertmannite, or goethite are found, as the former two may be masking the latter. Additionally, our findings suggest that outcrops on Mars with both goethite and ferrihydrite/schwertmannite VNIR signatures may have high relative abundances of goethite, or the goethite may exist in a coarsely crystalline phase.

1. Introduction

Over the past decade, satellite and landed missions to Mars have used visible- to near-infrared (VNIR) spectroscopy to identify and map minerals across the surface. Identifying the assemblages of minerals present in individual outcrops has allowed for the interpretation of past geochemical conditions (e.g., pH, Eh, temperature, and availability of cations and anions). In this way, a wide variety of low-temperature aqueous environments have been identified in ancient Martian terrains (e.g., Murchie et al., 2007, 2009; Langevin et al., 2005).

However, one of the major limitations of using VNIR spectroscopy to interpret past environments is how it responds to mineral assemblages. In reflectance spectroscopy, minerals are identified by the positions and shapes of absorption bands. In the near-infrared region, these bands are controlled by overtones and combinations of molecular vibrations: band positions depend on the crystal structure, bond lengths, and mineral composition; and band depths depend on the optical constants of the mineral at that wavelength, and the abundance of the mineral (e.g., Hapke, 1993). In other words: the depth of a mineral's absorption is not a direct function of the mineral's abundance.

If mixed with another mineral that has stronger optical constants at the same wavelengths, a mineral phase may be completely masked in the VNIR, even if it exists in greater abundance. For example, laboratory investigations by Chevrier et al. (2006) showed that a mixture of goethite, ferrihydrite, and siderite can mask up to 20 wt% siderite in the VNIR. Similarly, Muirhead et al. (2009) showed that hematite–magnetite–maghemite can mask ferrihydrite. This spectral masking effect can complicate the interpretation of environmental conditions on Mars, because key minerals can be obscured in the VNIR spectra.

An important set of minerals for interpreting past environmental conditions are the ferric oxyhydroxides and oxyhydroxysulfates: ferrihydrite ($Fe_2^{3+}O_3 \cdot 0.5H_2O$), goethite ($\alpha$-FeOOH), schwertmannite [$Fe_8O_8(OH)_6SO_4$], and jarosite [$KFe_3(SO_4)_2(OH)_6$]. These minerals have been identified at several locations on the Martian surface, including Mawrth Vallis (ferrihydrite, goethite, and jarosite, Farrand et al., 2009), the Mars Pathfinder landing site (ferrihydrite–schwertmannite mixtures in soil, Bishop et al., 1998), Aram Chaos (ferrihydrite–schwertmannite, Liu et al., 2012), and Meridiani Planum (schwertmannite, Farrand et al., 2007; Bibring et al., 2006; Klingelhöfer et al., 2005).

* Corresponding author. Tel.: +1 610 526 5116; fax: +1 610 526 5086.
E-mail address: scull@brynmawr.edu (S. Cull).

http://dx.doi.org/10.1016/j.epsl.2014.06.045
0012-821X/

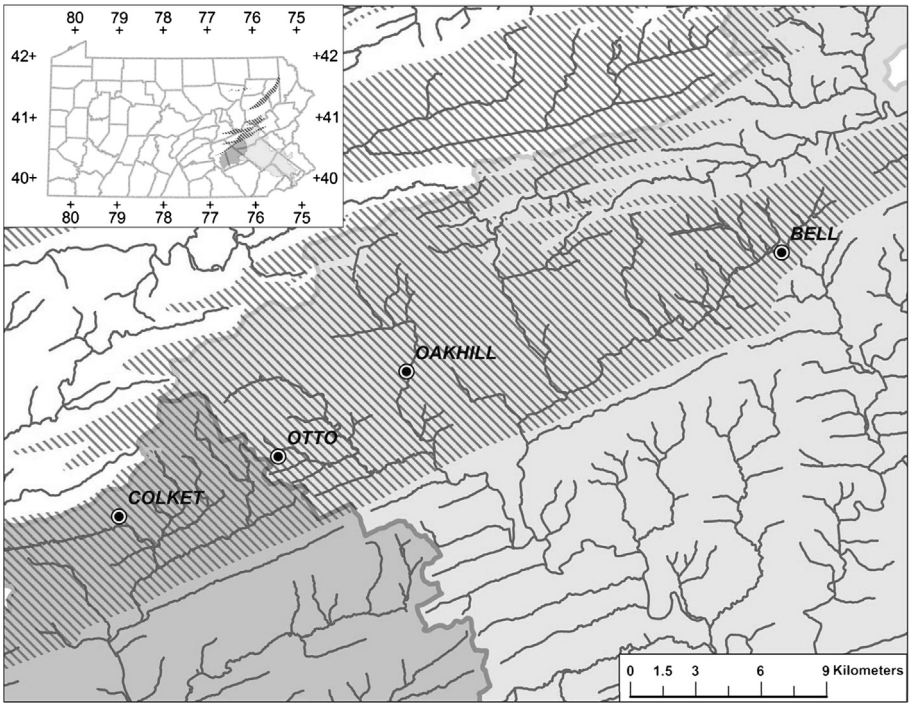

Fig. 1. Primary drainage basins and notable acid mine drainage (AMD) sites in the Southern Anthracite Coalfield, Pennsylvania. Shaded areas show different watersheds associated with each AMD site. Hachures indicate areas underlain by coal-bearing rocks.

The ferric oxyhydroxide and oxyhydroxysulfate minerals are of particular interest to our understanding of past and present Martian environments for several reasons. First, they are markers of liquid water and oxidizing conditions. Both geochemical modeling (e.g., Tosca et al., 2005) and laboratory experiments (e.g., King and McSween, 2005; Tosca et al., 2008) have shown that these hydrous minerals can form as aqueous alteration products of basalt and volcanic ash. Second, they can serve as markers of environmental conditions at their time of formation. For example, most ferrihydrite forms at low temperatures ($<25\,^{\circ}C$) at pH >3; schwertmannite forms in acid–sulfate environments with a pH 2.8–4.5; and goethite forms over a range of conditions (e.g., Bigham et al., 1996). Also, because these three minerals can be genetically linked (ferrihydrite and schwertmannite can co-precipitate in some circumstances, and both can re-crystallize into goethite), the exact assemblages and stratigraphic relationships of these minerals can provide insight into changing aqueous processes and environments at these locations on Mars. Finally, although ferric oxyhydroxide and oxyhydroxysulfate minerals can be synthesized inorganically, microbial processes commonly are associated with the oxidation of ferrous iron and the precipitation of these minerals from aqueous solutions in Earth environments (Bigham et al., 1990, 1992; Nordstrom and Alpers, 1999; Nordstrom, 2000).

Nevertheless, environmental interpretations on the basis of VNIR spectra are only useful to the extent that we can estimate mineral distributions in geologic and geographic context. Because they form in specific, but potentially diverse environments – and often are produced together or transformed from one another – iron-bearing minerals likely occur on Mars as mixtures with ferrihydrite, schwertmannite, and goethite. Interpretations about past and present environments would be hindered if an important mineral phase were spectrally masked.

Here, we analyze ferrihydrite–schwertmannite–goethite mixtures that naturally precipitate in abandoned mine drainage (AMD) systems in southeastern Pennsylvania. We use X-ray diffractometer (XRD) data to assess the presence of the three mineral phases, and a field VNIR spectrometer to record corresponding spectra of the mixtures. Geochemical data on the aqueous and surface environment at each sampling site are presented, and the results discussed in the context of ferrihydrite–schwertmannite–goethite mixtures on Mars.

2. Material and methods

2.1. Sampling sites

Samples were obtained from selected AMD sites in Pennsylvania's Southern Anthracite Field in November 2012 (Fig. 1). The coalfield is dominated by the Pennsylvanian-Age Llewellyn and Pottsville Formations: sandstone, siltstone, and conglomerates interbedded with ~30 coal beds, each about 1–4 m thick (e.g., Wood et al., 1968; Way, 2000). The Llewellyn and Pottsville coal beds were extensively mined during the 1800–1960s, resulting in a legacy of abandoned underground mines and waste rock piles. Pyrite and other sulfides in the exposed coal beds and host rocks oxidized during exposure to the atmosphere and, now, the oxidation products continue to leach from the flooded, abandoned mines, leading to extensive stream contamination. The contaminated streams have elevated concentrations of dissolved Fe that oxidizes along the flow path and forms ochreous precipitates, including ferrihydrite, schwertmannite, and goethite (Fig. 2). Contaminated local streams that drain the Southern Anthracite Field include Swatara Creek (Cravotta and Bilger, 2001; Cravotta et al., 2010), which is a tributary of the Susquehanna River, Wabash Creek, which feeds into the Little Schuylkill River (Cravotta, 2008b), plus the headwaters of the Schuylkill River (Cravotta and Ward, 2008), Mill Creek (Cravotta and Nantz, 2008), and the West Branch Schuylkill River (Cravotta et al., 2014), which are major tributaries of the upper Schuylkill River.

Several AMD systems that represented different aqueous environments were selected for analysis:

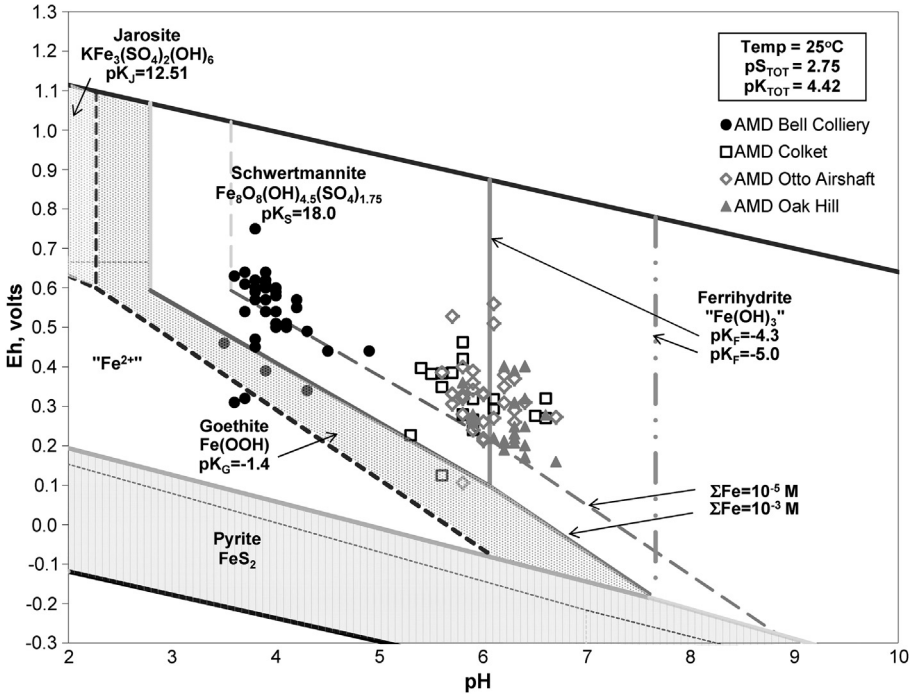

Fig. 2. Eh–pH diagram showing stabilities of commonly reported minerals in AMD systems and measured Eh and pH for four AMD systems in Pennsylvania. Data on Eh and pH for the AMD systems in Pennsylvania were measured on various dates during 1997–2012. See Fig. 1 for location of AMD systems. Thermodynamic data used to construct the stability boundaries from the WATEQ4F data base (Ball and Nordstrom, 1991) and Bigham et al. (1996).

1. ***Bell Colliery Drift, Schuylkill Township, Schuylkill County, PA:*** Discharge from an abandoned drift mine and waste rock pile, undergoing passive remediation with downflow limestone beds and aerobic wetlands since 2003. Untreated water exiting the collapsed drift is oxic (DO >6 mg/L) and net acidic with pH 3.5–4.3 and moderate levels of dissolved Al, Fe, and Mn (1–6 mg/L) and SO_4 (81–190 mg/L) (Cravotta and Ward, 2008). This discharge flows into the Schuylkill River, within meters of the river's headwaters, which caused the environmental protection agency (EPA) to name Bell Colliery as one of the highest priority AMD systems for remediation in the Schuylkill Watershed.
2. ***Otto Colliery Airshaft, Branchdale, Reilly Township, Schuylkill County, PA:*** Discharge from an abandoned shaft and associated spoil pile, undergoing passive remediation with aerobic wetlands since 2005. At the source of the discharge, the water exiting the shaft is suboxic (DO <2 mg/L) and net alkaline with pH 5.7–6.1 and moderate to high levels of Fe (3–16 mg/L), Mn (2–3 mg/L), and SO_4 (190–370 mg/L) (Cravotta, 2007). Discharge from the shaft flows into the Muddy Branch, which joins the West Branch of the Schuylkill River, then the West Branch, then the Schuylkill River itself. In 2000, the EPA named the Otto Airshaft as one of the more severe sources of pollution to the West Branch River.
3. ***Oak Hill Borehole, Minersville, Schuylkill County, PA:*** Discharge from several boreholes from 25 to 30 m deep is undergoing partial remediation with an open limestone channel since 2002. Untreated water from the Oak Hill Boreholes is suboxic and net alkaline with pH 5.8–7.0 and high concentrations of Fe (12–21 mg/L), Mn (3.1–4.5 mg/L), and SO_4 (360–450 mg/L) and is a major source of base flow and metals loading to the West Branch Schuylkill River (Cravotta et al., 2014).
4. ***Colket Mine Water Pool, Donaldson Village, Schuylkill County, PA:*** An abandoned mine shaft, unremediated. The discharge issues from an underground tunnel, then flows 200 m down to Good Spring Creek. The untreated discharge is suboxic and net acidic with pH 5.8 and high concentrations of Fe (23 mg/L) and moderate concentrations of Mn (1.6 mg/L) and SO_4 (160 mg/L) (Cravotta, 2010). Kirby and Cravotta (2005) explain that the pH of a net acidic discharge, such as that from the Colket Tunnel, ultimately will decrease to low values (<4.5) after complete oxidation of the dissolved Fe in the effluent.

At the time of sediment sampling in 2012, flow rate and water-chemistry data were collected, including pH, specific conductance (SC), temperature, redox potential (Eh), and dissolved oxygen (DO). To characterize the environmental conditions for sediment (mineral precipitates) accumulation, the pH and Eh data were combined with other such data that had been measured at these sites on various dates during 1997–2012 (Williams et al., 2002; Cravotta, 2008a, 2010; Cravotta and Ward, 2008; Cravotta et al., 2014). The pH and Eh were determined by use of a combination Pt and Ag/AgCl electrode with a pH sensor. The electrode was calibrated in pH 2.0, 4.0, and 7.0 buffer solutions and in ZoBell's solution daily when used. Values for Eh were corrected to 25 °C relative to the standard hydrogen electrode in accordance with methods of Nordstrom (1977). Sediment samples (approximately 0.5–1 L each) were collected in polypropylene bottles. Samples included floc precipitates and precipitates formed on rock surfaces. VNIR spectra were obtained at time of sampling using a field spectrometer (described below). Floc samples were then wet sieved through a 70-mesh stainless steel sieve and allowed to dry before analysis. Rock coatings were allowed to dry on rocks.

2.2. XRD analysis

To confirm composition, samples were analyzed with X-ray powder diffraction, using Bryn Mawr College's Rigaku Ultima IV X-ray Diffractometer. The XRD has a Cu target and graphite monochromator, and was operated at 3.0 kW between 5 and 80° 2-theta, with a scan rate of 1°/min at a step interval width of 0.02° and a count time of 1 s. Samples were ground to a fine powder in an acetone solution by using an agate mortar and pestle, and allowed to dry on a silicon slide. VNIR spectra of each sam-

ple were taken after preparation for XRD analysis and immediately before XRD measurements were taken to account for any phase changes that might have occurred due to sample preparation or time. No differences were found.

X-ray diffractograms were analyzed from XRD libraries by using Material Data Incorporated's JADE software, and were compared to the published d-spacings of intensity peaks. Schwertmannite was identified by its eight peaks: 4.95, 3.36, 2.56, 2.25, 1.95, 1.67, 1.52, and 1.45 Å, of which the 2.56 and 1.52 Å peaks are most diagnostic (Loan et al., 2004). "Ferrihydrite" actually comprises a group of minerals of varying states of disorder. At its most disordered (also called hydrous ferric oxide), XRD patterns of ferrihydrite show two broad scattering bands that correspond to d-spacings of 2.59 and 1.49 Å. At its most crystalline, XRD patterns of six-line ferrihydrite show six narrower scattering bands, corresponding to d-spacings of 4.4, 2.5, 2.24, 1.97, 1.72, and 1.47 Å. The two-line variety is most common; six-line ferrihydrite is rarely reported in AMD settings. Goethite has peaks corresponding to 4.18, 2.68, 2.59, 2.45, 2.19, 1.71, 1.56, and 1.51 Å, of which the three most characteristic are 4.18, 2.59, and 2.452 (Cornell and Schwertmann, 2003).

2.3. Spectral analysis

VNIR spectra of each sample were taken by using Bryn Mawr College's ASD FieldSpec Pro visible- to near-infrared spectrometer. The spectrometer covers a spectral range from 0.35 to 2.5 μm at a sampling interval of 1.277 nm for the 0.35–1.0 μm region and 2 nm for the 1.0–2.5 μm region, and a spectral resolution of 3 nm at 0.7 μm and 10 nm at 1.4 and 2.1 μm. The spectrometer was calibrated by using a Spectralon disk. Samples were illuminated with a high-intensity contact probe with halogen bulb. Three spectra were taken for each sample: one immediately after sampling (in the field), one after drying the samples in the lab, and one after preparing samples for the XRD. This was done to observe any phase changes due to time, drying, or removal from original environment. No differences were observed.

Ferrihydrite, goethite, and schwertmannite are all iron-bearing, hydrated or hydroxylated minerals, and so share several similar spectral features in the VNIR (e.g., Morris et al., 1985; Sherman, 1990; Scheinost et al., 1998). Their signatures can be distinguished by variations in absorptions.

Iron dominates spectra between 0.4 and 1.0 μm, described in detail by Cornell and Schwertmann (2003). A single electron transition [^4E; $^4A_1 \leftarrow {}^6A_1$] produces an absorption in the ~0.42 μm range: at 0.410 (ferrihydrite), 0.413 (goethite), and 0.416 μm (schwertmannite). An electron pair transition in iron ($^4T_1 + {}^4T_1$) $\leftarrow$ ($^6A_1 + {}^6A_1$) results in a strong absorption near ~0.49 μm: 0.492 (ferrihydrite), 0.488 (goethite), and 0.489 μm (schwertmannite). Another single-electron transition ($^4T_2$) $\leftarrow$ ($^6A_1$) produces a weaker absorption near ~0.7 μm: at 0.716 (ferrihydrite), 0.665 (goethite), and 0.655 μm (schwertmannite). A third single-electron transition ($^4T_1$) $\leftarrow$ ($^6A_1$) produces a broad absorption at ~0.95 μm: at 0.972 (ferrihydrite), 0.953 (goethite), and 0.952 μm (schwertmannite).

Between 1.0–2.5 μm, bound and absorbed H_2O and OH groups produce three major spectral features, as described by Ling and Wang (2010). First, the 2ν overtone of the OH stretch produces an absorption near 1.4 μm: 1.427 (ferrihydrite), 1.417 (goethite), and 1.4525 μm (schwertmannite). Second, a combination of the fundamental bending (ν_2) and asymmetric stretching (ν_3) modes in bound H_2O molecules produces an absorption band near 1.9 μm: 1.923 (ferrihydrite), 1.950 (goethite), and 1.953 μm (schwertmannite). Finally, the asymmetric and symmetric fundamental O–H stretches near 2.8 μm and the H_2O bend overtone near 3.1 μm combine to make a deep absorption centered near 3.0 μm. This absorption produces a characteristic negative slope in the spectra of ferrihydrite, goethite, and schwertmannite between ~2.0 and 2.5 μm.

Additionally, each mineral displays its own characteristic spectral features. Ferrihydrite has a "shoulder" (slope break) at 2.28 μm, goethite an absorption at 2.4–2.5 μm, and schwertmannite a shoulder at ~2.53 μm. These minerals can be distinguished from each other by the band centers of their shared absorptions and/or the unique absorptions each has.

AMD systems often have additional mineral phases related to ferrihydrite, schwertmannite, and goethite, including jarosite, gypsum, amorphous aluminum oxides and hydroxysulfates, and lepidocrocite [γ-FeO(OH)] (e.g. Nordstrom and Alpers, 1999). These minerals are also detectable spectrally. Lepidocrocite and jarosite share the ~0.5 and ~1.0 μm iron transitions, and the 1.4 and 1.9 μm hydration bands. However, jarosite also has a combination OH-stretch and Fe–OH bend that create a diagnostic absorption at 2.27 μm. Lepidocrocite's ~1.0 μm absorption is shifted to lower wavelengths (0.933 μm) and its ~0.7 μm absorption appears usually as a shoulder at 0.67 μm. Gypsum has a characteristic triplet at 1.4–1.54 μm, and strong absorptions at 1.75 and 1.94 μm, and a doublet at 2.21 and 2.23 μm. The amorphous aluminum phases that are often found in AMD systems vary in spectral character, but lack the characteristic iron transitions. Spectra of mineral mixtures from the sample sites were inspected for evidence of these mineral phases as well, by using these absorption band positions as indicators.

3. Results

Different mineral assemblages were identified for the four sites:

3.1. Oak Hill Borehole

At the Oak Hill Borehole, ochreous precipitates form on the discharge channel and submerged rock surfaces within the borehole where the water emerges. XRD analyses show that the precipitates closest to the borehole are goethite (Fig. 3), without ferrihydrite or schwertmannite. VNIR spectra show typical goethite absorptions and no evidence of ferrihydrite or schwertmannite, consistent with the XRD results.

3.2. Bell Colliery

Ochre samples collected upstream and downstream of Bell Colliery's limestone treatment ponds were brownish–red precipitates, which XRD analysis showed to be a mixture of goethite and schwertmannite (Fig. 3). The XRD patterns showed peaks associated with goethite (including the characteristic triple peak at 34.6, 34.7, and 36.6° 2-theta) and the broader peaks associated with schwertmannite. The goethite peaks in these samples also were broadened, an effect associated with nanophase goethite (e.g., Schwertmann et al., 1985). Previous samples of the precipitate at the sampled locations also had been identified as goethite and schwertmannite (Williams et al., 2002).

VNIR spectra of the two samples from Bell Colliery show only schwertmannite (Fig. 4), including a shoulder at 0.655 μm, a broad absorption centered at 0.952 μm, 2ν overtone of the OH stretch at 1.453 μm, and ν_2–ν_3 combination at 1.953 μm. Despite the clear signature of goethite in XRD analyses of these samples, goethite's characteristic 0.665 μm and 2.4 μm absorptions do not appear in the VNIR, nor do the schwertmannite absorptions appear to be affected by the presence of goethite.

3.3. Colket Mine

XRD analysis of precipitates at the Colket discharge indicate the precipitate is composed of ferrihydrite and goethite (Fig. 3). The

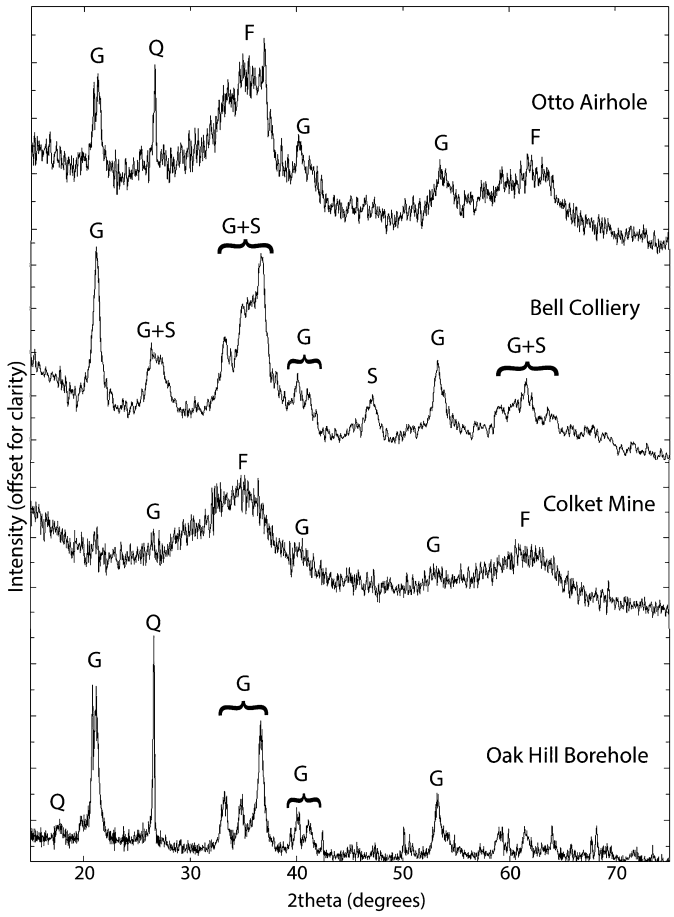

Fig. 3. X-ray diffractograms of precipitate samples from four AMD systems in southeastern Pennsylvania. Peaks associated with important minerals are identified: F for ferrihydrite, G for goethite, S for schwertmannite, and Q for quartz.

VNIR spectra of the precipitates show only ferrihydrite (Fig. 4). Samples collected in 1997 from the Colket Mine discharge also contained goethite but with schwertmannite instead of ferrihydrite (Williams et al., 2002), perhaps due to seasonal variations in water quality or increased pH during the 11 yr gap between the two studies.

3.4. Otto airshaft wetlands

Samples collected downstream of the Otto wetlands, several hundred meters below the airshaft, were caked in brownish–red precipitates, which XRD analysis identified as mixtures of two-line ferrihydrite and goethite (Fig. 3). The two-line ferrihydrite showed in the XRD analyses as distinctive broad peaks, centered at 34.6 and 62.2°-2-theta. The ferrihydrite peaks were so broad and intense that they nearly masked the goethite peaks, which again appeared broadened, perhaps due to the presence of nanophase goethite. Possibly due to the same effect, samples collected in 1997 at the Otto Mine discharge were identified only as two-line ferrihydrite at the airshaft and six-line ferrihydrite downstream (Williams et al., 2002).

VNIR spectra of the Otto wetlands precipitates show only ferrihydrite (Fig. 4). The spectra have absorptions at 0.972, 1.427, and 1.923 μm – all band centers characteristic of ferrihydrite. Despite the presence of goethite in XRD of these mixtures, the VNIR band centers for the ferrihydrite appear unaffected by goethite. Ferrihydrite's 0.972 μm absorption is not shifted to shorter wavelengths

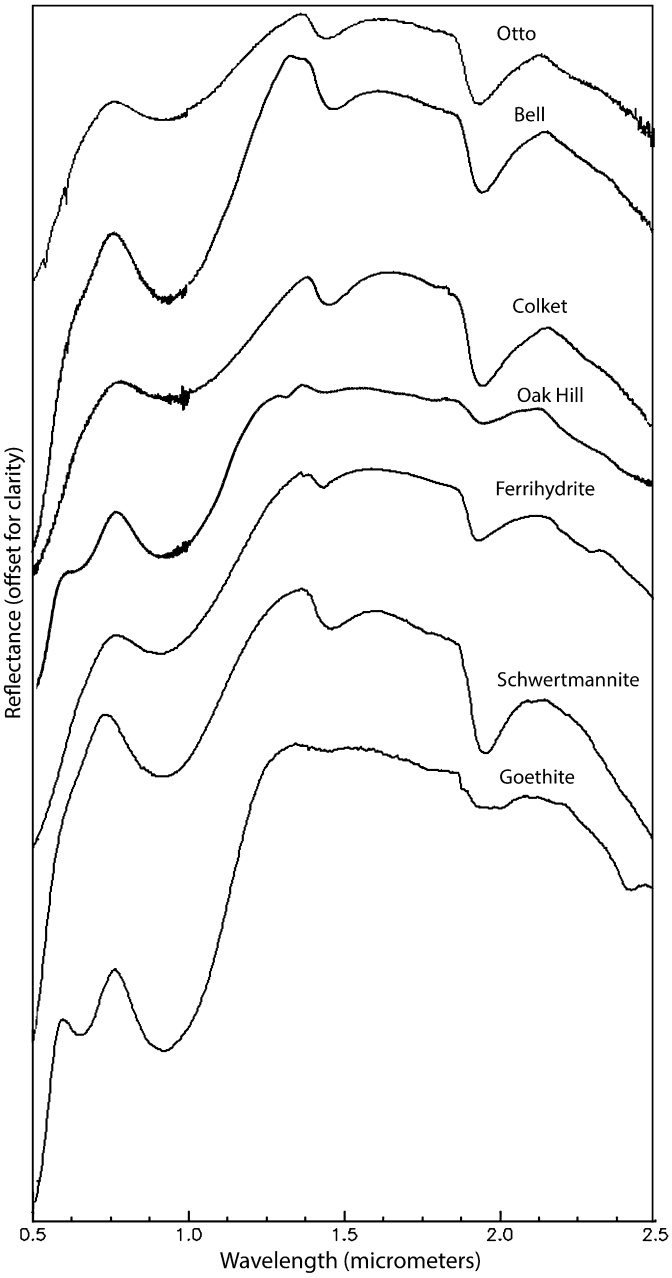

Fig. 4. VNIR spectra of precipitate samples from four southeastern Pennsylvania AMD systems, compared to laboratory spectra of ferrihydrite, schwertmannite, and goethite standards.

to reflect goethite's 0.952 μm absorption, and the spectra are lacking goethite's distinctive 0.665 and 2.4 μm absorptions.

Across all AMD sites examined here, mixtures of ferrihydrite and goethite appear as only ferrihydrite in VNIR (Fig. 4), and mixtures of schwertmannite and goethite appear as only schwertmannite in the VNIR (Fig. 4). Despite potentially overlapping stability fields indicated by the measured Eh and pH of the aqueous samples for Colket, Otto, and Oak Hill AMD effluents (Fig. 2), ferrihydrite and schwertmannite were not observed together at any site. On the basis of thermodynamic stability, goethite would be the most stable phase at all the sites sampled, with schwertmannite and ferrihydrite formed as intermediate phases. No site showed XRD or VNIR evidence of other AMD-related minerals discussed here, such as jarosite.

4. Discussion

Ferrihydrite, schwertmannite, and goethite have been reported in remote sensing data at several locations across Mars. Because these minerals are often used as environmental indicators, and because they likely occur in mixtures, it is important to understand how mixing affects the spectral signatures observed from orbit and from landed missions.

Our survey of AMD systems in southeastern Pennsylvania shows that ferrihydrite and schwertmannite can both spectrally mask goethite. At Bell Colliery, XRD analysis showed that both goethite and schwertmannite are present, but only schwertmannite appears in the VNIR. At both Otto and Colket, XRD analysis shows that both ferrihydrite and goethite are present, but VNIR spectra show only ferrihydrite.

This masking in natural samples could be caused by relative grain sizes. The XRD goethite peaks appear broadened in these samples, an effect often attributed to the nanocrystalline phase of goethite (indicating a grain size of 10–100 nm). Nanophase goethite is common in acid–sulfate environments on Earth (e.g., Waychunas et al., 2005), and is hypothesized to be present on Mars. Laboratory experiments simulating goethite precipitation under Martian conditions show that it usually forms as a nanocrystalline phase (e.g., Tosca et al., 2008), perhaps due to rapid nucleation during precipitation or slow growth kinetics (Cornell and Schwertmann, 2003). Small grain size at the AMD sites could decrease the absorption features of goethite such that the presence of other hydrated and hydroxylated minerals could mask its presence.

Multiple phases generally could be anticipated under the Eh–pH conditions reported for these AMD sites, consistent with the overlapping stability fields for schwertmannite, ferrihydrite, and goethite (Fig. 2). Schwertmannite and ferrihydrite that precipitated from solution ultimately may transform to goethite (e.g. Bigham et al., 1996). Nevertheless, goethite was the only phase identified at Oak Hill, and schwertmannite was not observed with ferrihydrite and goethite at Otto or Colket.

4.1. Implications for Mars

Iron-bearing oxyhydroxides and oxyhydroxysulfates have been identified using VNIR spectroscopy at several locations on Mars, including ferrihydrite, goethite, and jarosite at Mawrth Vallis (Farrand et al., 2009), and schwertmannite at Aram Chaos (Liu et al., 2012).

4.1.1. Aram Chaos

Aram Chaos displays a complex stratigraphy. Lichtenberg et al. (2010) mapped the stratigraphic column by using CRISM data, identifying an underlying chaos basement, draped by a layer of monohydrated sulfates mixed with an unnamed hydroxylated ferric sulfate, topped by a layer of monohydrated sulfates mixed with nanophase iron oxides, and capped by a much younger unit. This younger unit has been the subject of several studies, and has been mapped as crystalline hematite (Christensen et al., 2001) mixed with goethite/ferrihydrite/schwertmannite (Massé et al., 2008) and a polyhydrated sulfate (Lichtenberg et al., 2010; Noe Dobrea et al., 2008) that may be starkeyite (Liu et al., 2012).

Given that our naturally-precipitated ferrihydrite–goethite mixtures successfully masked goethite in the VNIR, the VNIR-spectral identification of all three in the Aram Chaos capping unit is interesting. The mapping may point to very abundant goethite relative to ferrihydrite/schwertmannite – perhaps as ferrihydrite/schwertmannite have recyrstallized into goethite over time. Alternatively, because it appears to be the nanocrystalline form of goethite that is spectrally masked in our natural samples, the Aram Chaos goethite may exist in a more coarsely crystalline phase.

The Aram Chaos capping unit has been interpreted as a result of acid–sulfate weathering and evaporation, driven by periods of rising groundwater (e.g., Liu et al., 2012). If so, the system closely resembles laboratory experiments conducted by Tosca et al. (2008), which found that goethite co-precipitating with schwertmannite under such conditions formed nanocrystalline phases too small even to be resolved under SEM examination. Taken together with our findings, this suggests that goethite may dominate the Aram Chaos capping unit, with only minor amounts of ferrihydrite/schwertmannite. Because ferrihydrite/schwertmannite both age to goethite over time in the presence of water, the dominance of goethite in the Aram Chaos capping unit could indicate that the unit was exposed to prolonged liquid water after the initial precipitation of schwertmannite/ferrihydrite.

4.1.2. Mawrth Vallis

Mawrth Vallis is the oldest of the outflow channels that empty into Chryse Planitia. It carves through Noachian-age layers of light-toned materials that have a mineralogically-rich stratigraphy: a layer of Fe–Mg smectites, overlain by a hydrated layer that includes hydrated silica, montmorillonite, and kaolinite (Bishop et al., 2008). Isolated to one segment of the valley, Farrand et al. (2009) reported a layer rich in K-jarosite, goethite, and ferrihydrite, stratigraphically above the Fe/Mg-smectite layer and of uncertain stratigraphy relative to the Al-phyllosilicate layer.

As with Aram Chaos, the presence of ferrihydrite and goethite in the VNIR spectra could indicate that the goethite is abundant relative to the ferrihydrite, or that the goethite exists in a coarsely crystalline phase. The latter would argue against the hypothesis put forward by Farrand et al. (2009) that the goethite formed by transformation from schwertmannite, since laboratory experiments have shown that this transformation produces nanocrystalline goethite (e.g., Tosca et al., 2008). This would argue for abundant goethite at the Mawrth Vallis jarosite outcrop, relative to the ferrihydrite that is present.

5. Conclusions

XRD and VNIR analyses of natural mixtures of ferrihydrite–goethite–schwertmannite from AMD sites show that ferrihydrite and schwertmannite can mask goethite in VNIR spectra. The effect is most likely more acute for nanophase goethite. These findings suggest that care should be taken in interpreting environments on Mars where ferrihydrite, schwertmannite, or goethite are found, as the former two may be masking the latter. Additionally, our findings suggest that outcrops on Mars with both goethite and ferrihydrite/schwertmannite VNIR signatures may have high relative abundances of goethite, or the goethite may exist in a coarsely crystalline phase. Future laboratory work is needed to understand the relative abundances of ferrihydrite/goethite needed to spectrally mask goethite at various grain sizes.

Acknowledgements

The authors would like to thank the Schuylkill Headwaters Association and Schuylkill Conservation District for their field assistance, particularly Wayne Lehman and William Reichert. We also thank the Bryn Mawr College Praxis Program and Summer Science Program, which provided funding and support for student involvement in this project, and EunJi Yun and Misha Sims for help with sample preparation. Finally, we thank Jerry Bigham and two anonymous reviewers for feedback that improved the quality of this manuscript. Any use of trade, firm, or product names is for descriptive purposes only and does not imply endorsement by the U.S. Government.

References

Ball, J.W., Nordstrom, D.K., 1991. User's manual for WATEQ4F with revised data base. U.S. Geol. Surv. Open-File Rep. 91 (183). 189 p.

Bibring, J.-P., Langevin, Yves, Mustard, John F., Poulet, François, Arvidson, Raymond, Gendrin, Aline, Gondet, Brigitte, Mangold, Nicolas, Pinet, P., Forget, F., The OMEGA team, 2006. Global mineralogical and aqueous Mars history derived from OMEGA/Mars Express data. Science 312, 400–404. http://dx.doi.org/10.1126/science.1122659.

Bigham, J.M., Schwertmann, U., Carlson, L., Murad, E., 1990. A poorly crystalline oxyhydroxysulfate of iron formed by bacterial oxidation of Fe(II) in acid mine waters. Geochim. Cosmochim. Acta 54, 2743–2758. http://dx.doi.org/10.1016/0016-7037(90)90009-A.

Bigham, J.M., Schwertmann, U., Carlson, L., 1992. Mineralogy of precipitates formed by the biogeochemical oxidation of Fe(II) in mine drainage. In: Skinner, J., Fitzpatrick, R. (Eds.), Biomineralization Processes of Iron and Manganese – Modern and Ancient Environments. Catena Verlag.

Bigham, J.M., Schwertmann, U., Traina, S.J., Winland, R.L., Wolf, M., 1996. Schwertmannite and the chemical modeling of iron in acid sulfate waters. Geochim. Cosmochim. Acta 60, 2111–2121.

Bishop, J.L., Scheinost, A., Bell, J.F., Britt, D., Johnson, J.R., Murchie, S., 1998. Ferrihydrite–schwertmannite–silicate mixtures as a model of Martian soils measured by Pathfinder. Lunar and Planetary Science Conference. Abstract #1803.

Bishop, J., Noe Dobrea, E.Z., McKeown, N., Parente, M., Ehlman, B., Michalski, J.R., Milliken, R., Poulet, F., Swayze, G., Mustard, J., 2008. Phyllosilicate diversity and past aqueous activity revealed at Mawrth Vallis, Mars. Science 321, 830–833. http://dx.doi.org/10.1126/science.1159699.

Chevrier, V., Roy, R., Le Mouelic, S., Borschneck, D., Mathe, P., Rochette, P., 2006. Spectral characterization of weathering products of elemental iron in a Martian atmosphere: implications for Mars hyperspectral studies. Planet. Space Sci. 54, 1034–1045. http://dx.doi.org/10.1016/j.pss.2005.12.019.

Christensen, P.R., Malin, M.C., Morris, R.V., Bandfield, J.L., Lane, M.D., 2001. Martian hematite mineral deposits: remnants of water-driven processes on early Mars. J. Geophys. Res. 106, 23,873–23,885.

Cornell, R.M., Schwertmann, U., 2003. The Iron Oxides: Structures, Properties, Reactions, Occurrences, and Uses. Wiley-VCH, Berlin.

Cravotta III, C.A., 2007. Passive aerobic treatment of net-alkaline, iron-laden drainage from a flooded underground anthracite mine, Pennsylvania, USA. Mine Water Environ. 26, 128–149. http://dx.doi.org/10.1007/s10230-007-0002-8.

Cravotta III, C.A., 2008a. Dissolved metals and associated constituents in abandoned coal-mine discharges, Pennsylvania, USA: 1. Constituent concentrations and correlations. Appl. Geochem. 23, 166–202. http://dx.doi.org/10.1016/j.apgeochem.2007.10.011.

Cravotta III, C.A., 2008b. Laboratory and field evaluation of a flushable oxic limestone drain for treatment of net-acidic drainage from a flooded anthracite mine, Pennsylvania, USA. Appl. Geochem. 23, 3404–3422. http://dx.doi.org/10.1016/j.apgeochem.2008.07.015.

Cravotta III, C.A., 2010. Abandoned mine drainage in the Swatara Creek Basin, Southern Anthracite Coalfield, Pennsylvania, USA – 2. Performance of passive-treatment systems. Mine Water Environ. 29, 200–216. http://dx.doi.org/10.1007/s10230-010-0113-5.

Cravotta III, C.A., Bilger, M.D., 2001. Water-quality trends for a stream draining the Southern Anthracite Field, Pennsylvania. Geochem., Explor. Environ. Anal. 1, 33–50. http://dx.doi.org/10.1144/geochem.1.1.33.

Cravotta III, C.A., Nantz, J.M., 2008. Quantity and quality of stream water draining mined areas of the upper Schuylkill River basin, Schuylkill County, Pennsylvania, 2005–2007. Am. Soc. Min. Reclam., 223–252.

Cravotta III, C.A., Ward, S.J., 2008. Downflow limestone beds for treatment of net-acidic, oxic, iron-laden drainage from a flooded anthracite mine, Pennsylvania, USA – field evaluation. Mine Water Environ. 27, 67–85. http://dx.doi.org/10.1007/s10230-008-0029-5.

Cravotta III, C.A., Brightbill, R.A., Langland, M.J., 2010. Abandoned mine drainage in the Swatara Creek Basin, Southern Anthracite Coalfield, Pennsylvania, USA – 1. Streamwater-quality trends coinciding with the return of fish. Mine Water Environ. 29, 176–199. http://dx.doi.org/10.1007/s10230-010-0112-6.

Cravotta III, C.A., Goode, D.J., Bartles, M.D., Risser, D.W., Galeone, D.G., 2014. Surface-water and groundwater interactions in an extensively mined watershed, Upper Schuylkill River, Pennsylvania, USA. Hydrol. Process. 28, 3574–3601. http://dx.doi.org/10.1002/hyp.9885.

Farrand, W.H., Bell III, J.F., Johnson, J.R., Joliff, B.L., Knoll, A., McLennan, S., Squyres, S., Calvin, W., Grotzinger, J., Morris, R.V., Soderblom, J., Thompson, S., Walters, W., Yen, A., 2007. Visible and near-infrared multispectral analysis of rocks at Meridiani Planum, Mars, by the Mars Exploration Rover Opportunity. J. Geophys. Res. 112, E06S02. http://dx.doi.org/10.1029/2006JE002773.

Farrand, W.H., Glotch, T.D., Rice, J.W., Hurowitz, J.A., Swayze, G., 2009. Discovery of jarosite within the Mawrth Vallis region of Mars: implications for the geologic history of the region. Icarus 204, 478–488. http://dx.doi.org/10.1016/j.icarus.2009.07.014.

Hapke, B., 1993. Introduction to the Theory of Reflectance and Emittance Spectroscopy. Cambridge University Press, New York.

King, P., McSween, H., 2005. Effects of H_2O, pH, and oxidation state on the stability of Fe minerals on Mars. J. Geophys. Res. 110, E12S10. http://dx.doi.org/10.1029/2005JE002482.

Kirby, C.S., Cravotta III, C.A., 2005. Net alkalinity and net acidity 1: theoretical considerations. Appl. Geochem. 20, 1920–1940. http://dx.doi.org/10.1016/j.apgeochem.2005.07.002.

Klingelhöfer, G., DeGrave, E., Morris, R.V., Van Alboom, A., de Resende, V.G., De Souza, P.A., Rodinov, D., 2005. Mössabauer spectroscopy of Mars: goethite in the Columbia Hills at Gusev Crater. Hyperfine Interact. 166, 549–554. http://dx.doi.org/10.1007/978-3-540-49850-6_86.

Langevin, Y., Poulet, F., Bibring, J.P., Gondet, B., 2005. Sulfates in the North Polar region of Mars detected by OMEGA/Mars Express. Science 307, 1584–1586. http://dx.doi.org/10.1126/science.1109091.

Lichtenberg, K., Arvidson, R., Morris, R.V., Murchie, S.L., Bishop, J.L., Fernandez-Remolar, D., Mustard, J.F., Andrews-Hanna, J., Roach, L.H., 2010. Stratigraphy of hydrated sulfates in the sedimentary deposits of Aram Chaos, Mars. J. Geophys. Res. 115, E00D17. http://dx.doi.org/10.1029/2009JE003353.

Ling, Z.C., Wang, A., 2010. A systematic spectroscopic study of eight hydrous ferric sulfates relevant to Mars. Icarus 209, 422–433. http://dx.doi.org/10.1016/j.icarus.2010.05.009.

Liu, Y., Arvidson, R.E., Wolff, M.J., Mellon, M., Wang, A., Bishop, J., 2012. Lambert albedo retrieval and analysis over Aram Chaos from OMEGA hyperspectral imaging data. J. Geophys. Res. 117, E00J11. http://dx.doi.org/10.1020/2012J004056.

Loan, M., Cowley, J.M., Hart, R., Parkinson, G., 2004. Evidence of the structure of synthetic schwertmannite. Am. Mineral. 89 (11), 1735–1742.

Massé, M., Le Mouelic, S., Bouregeois, O., Combe, J.P., Le Deit, L., Sotin, C., 2008. Mineralogical composition, structure, morphology, and geological history of Aram Chaos crater fill on Mars derived from OMEGA Mars Express data. J. Geophys. Res. 113, E12006. http://dx.doi.org/10.1029/2008JE003131.

Morris, R.V., Lauer, H.V., Lawson, C.A., Gibson, E.K., 1985. Spectral and other physiochemical properties of submicron powders of hematite, maghemite, magnetite, goethite, and lepidocrocite. J. Geophys. Res. 90 (B4), 3126–3144. http://dx.doi.org/10.1029/JB090iB04p03126.

Muirhead, A.C., Bishop, J., McKeown, N., 2009. The VNIR spectral properties of iron oxide/hydroxide mixtures and application to iron oxides in the Mawrth Vallis region of Mars. Lunar and Planetary Science Conference. Abstract #1652.

Murchie, S.L., Arvidson, R., Bedini, P., Beisser, K., Bibring, J.P., Boldt, J., Cavender, P., The CRISM Team, 2007. Compact Reconnaissance Imaging Spectrometer for Mars (CRISM) on Mars Reconnaissance Orbiter (MRO). J. Geophys. Res. 112, E05S03. http://dx.doi.org/10.1029/2006JE002682.

Murchie, S.L., Mustard, J.F., Ehlmann, B., Milliken, R., Bishop, J., McKeown, N., Noe Dobrea, E., 2009. A synthesis of Martian aqueous mineralogy after 1 Mars year of observations from the Mars Reconnaissance Orbiter. J. Geophys. Res. 114, E00D06. http://dx.doi.org/10.1029/2009JE003342.

Noe Dobrea, E.Z., Poulet, F., Malin, M.C., 2008. Correlations between hematite and sulfates in the chaotic terrain east of Valles Marineris. Icarus 193, 516–534. http://dx.doi.org/10.1016/j.icarus.2007.06.029.

Nordstrom, D.K., 1977. Thermochemical redox equilibria of Zobell's solution. Geochim. Cosmochim. Acta 41, 1835–1841.

Nordstrom, D.K., 2000. Advances in the hydrochemistry and microbiology of acid mine waters. Int. Geol. Rev. 42, 499–515.

Nordstrom, D.K., Alpers, C.N., 1999. Geochemistry of acid mine waters. In: Plumlee, G.S., Logsdon, M.J. (Eds.), The Environmental Geochemistry of Mineral Deposits – Part A. Processes, Methods, and Health Issues. Rev. Econ. Geol. A 6, 133–160.

Scheinost, A.C., Chavernas, A., Barron, V., Torrent, J., 1998. Use and limitations of second-derivative diffuse reflectance spectroscopy in the visible to near-infrared range to identify and quantify Fe oxide minerals in soils. Clays Clay Miner. 46, 528–536.

Schwertmann, U.D., Cambier, P., Murad, E., 1985. Properties of goethites of varying crystallinity. Clays Clay Miner. 33 (5), 369–378.

Sherman, D.M., 1990. Crystal chemistry, electronic structures, and spectra of Fe sites in clay minerals. In: Coyne, L.M., McKeever, S.W.S., Drake, D.F. (Eds.), Spectroscopic Characterization of Minerals and their Surfaces. American Chemical Society, Washington, DC.

Tosca, N., McLennan, S., Clark, B., Grotzinger, J., Hurowitz, J., Knoll, A., Schroder, C., 2005. Geochemical modeling of evaporation processes on Mars: insight from the sedimentary record at Meridiani Planum. Earth Planet. Sci. Lett. 240, 122–148. http://dx.doi.org/10.1016/j.epsl.2005.09.042.

Tosca, N.J., McLennan, S.M., Dyar, M.D., Sklute, E.C., Michel, F.M., 2008. Fe oxidation processes at Meridiani Planum and implications for secondary Fe mineralogy on Mars. J. Geophys. Res. 113, E05005. http://dx.doi.org/10.1029/2007JE003019.

Way, J.H., 2000. Appalachian Mountain section of the Ridge and Valley Province. In: Schultz, C.H. (Ed.), The Geology of Pennsylvania. In: Pennsylvania Geological Survey, 4th Series, Special Publication, vol. 1, pp. 352–361.

Waychunas, G.A., Kim, C.S., Banfield, J.F., 2005. Nanoparticulate iron oxide minerals in soils and sediments: unique properties and contaminant scavenging mechanisms. J. Nanopart. Res. 7, 409–433. http://dx.doi.org/10.1007/s11051-005-6931-x.

Williams, D.J., Bigham, J.M., Cravotta III, C.A., Traina, S.J., Anderson, J.E., Lyon, G., 2002. Assessing mine drainage pH from the color and spectral reflectance of chemical precipitates. Appl. Geochem. 17, 1273–1286. http://dx.doi.org/10.1016/S0883-2927(02)00019-7.

Wood Jr., G.H., Trexler, J.P., Kehn, T.M., 1968. Geologic maps of anthracite-bearing rocks in the west-central part of the southern Anthracite Field, Pennsylvania, eastern area. U.S. Geological Survey, Miscellaneous Geologic Investigations. Map I-528. http://ngmdb.usgs.gov/Prodesc/proddesc_1360.htm.